ANALYSIS AND SIMULATION OF COLLISION AVOIDANCE TCAS ANTENNAS MOUNTED ON AIRCRAFT *

R. G. Rojas **K. S. Sampath** **W. D. Burnside**
The Ohio State University
ElectroScience Laboratory
1320 Kinnear Road,
Columbus, Ohio 43212

Abstract

Traffic-alert and Collision Avoidance systems (TCAS) are being developed by order of the Federal Aviation Administration (FAA) to assist aircraft pilots in mid-air collision avoidance. This paper discusses computer models developed to simulate the radiation patterns of TCAS arrays mounted on the fuselage of any aircraft. Computer models are also used to calculate and evaluate the errors in estimating the bearing of aircraft in the vicinity of a TCAS-equipped airplane. The performance of two TCAS systems mounted on a Boeing 737 aircraft are studied and compared.

1 Introduction

The Federal Aviation Administration (FAA) has ordered that all aircraft which can carry 30 or more passengers must be fitted with an advanced Traffic-alert Collision Avoidance System (TCAS) equipment by the end of 1991 [1]. Presently, there are three generations of this system, namely the TCAS I, II and III systems. The first system, known as the TCAS I, can only detect the presence of other aircraft in the vicinity of the TCAS-equipped aircraft but it cannot give pilots advice on what maneuvers to take to avoid a collision. The TCAS II system, which is in the production phase at the present time, has conflict resolution logic which can tell the pilot to climb, dive or maintain the same altitude to avoid collision. The TCAS III system, which is still in the experimental stage, can advise the pilot to turn right or left as well as climb or dive. To accomplish the latter task, the TCAS III system has to be able to accurately determine the bearing of other aircraft with respect to the TCAS-equipped aircraft. Note that in all three systems, it is necessary for the other aircraft to be fitted with a transponder to respond to the interrogation of the TCAS system. The TCAS III system can then determine the altitude, velocity, distance, and bearing of nearby transponder-equipped aircraft by interpreting the transponder return and measuring the time delay of the response [2]. More details about the TCAS III system can be found in [3, 4, 5] and will not be repeated here.

As stated in [6], there are many factors that adversely affect the performance of the TCAS III system in estimating the bearing of the surrounding aircraft. Note that it is not very difficult to predict the performance of the TCAS array by itself in determining

*This work was supported in part by NASA, Langley Research Center under Grant NSG 1498 to The Ohio State University.

the bearing of nearby aircraft; however, when it is mounted on the fuselage of an aircraft, it is much more difficult to predict the performance due to the distortion of the radiation pattern by the curvature of the fuselage, and by the scattering of the wings, engines, vertical and horizontal stabilizers, and other antennas located on the aircraft. The cost of making full scale measurements and of evaluating these systems under actual flight conditions is very high and time consuming. Therefore, there is a need for alternative ways to evaluate and study the performance of these systems when they are mounted on the fuselage of an aircraft. One well known technique is to use scale models to make the measurements [7]. Another alternative is to use computer models to calculate the radiation patterns in the near or far field.

The main purpose of this paper is to present the theoretical models that have been developed to study the effect of the aircraft itself on the performance of the TCAS III system in estimating the bearing of nearby aircraft. These theoretical models are general enough that with the help of a digital computer, the TCAS arrays can be mounted on any type of aircraft; however, in this paper the results for only two aircraft, namely, the Boeing 727 and Boeing 737 will be presented. The computer models presented here are also very useful in the study of the proper placement of the TCAS array on the fuselage of an aircraft such that the best system performance is obtained.

The theoretical analysis can be divided into two main parts. The first part is the calculation of the field radiated by each single element of the TCAS array (taking into account mutual coupling) mounted on the fuselage of an aircraft. To accomplish this task, the Ohio State University Aircraft Code is used [8, 9]. This code, which can be used to analyze the near and far zone radiation patterns of antennas mounted on an aircraft or any other similar geometry, is based on the Uniform Geometrical Theory of Diffraction [9]. It has been used extensively and successfully in the past to study a variety of problems such as the Microwave Landing System (MLS) [10, 11, 12] and is widely used by the aerospace industry. All the details about this code and the theoretical background can be found in [8, 9]. It is sufficient to state that the fuselage is modeled by a composite ellipsoid (generated by joining two ellipsoids). This gives one, the flexibility of modeling a wide variety of aircraft fuselages. Other structural components such as wings, stabilizers, engines, etc., are modeled by flat plates.

The second part of the theoretical analysis is to properly combine the array element patterns to generate the various TCAS array radiation patterns. These radiation patterns are then used as inputs to a number of algorithms to estimate the bearing of nearby aircraft. Obviously, there are a number of ways to do bearing calculations. In this paper, two systems which have been built and are being tested will be studied and compared. Both systems have circular array antennas, one using eight monopoles and the other just four. The eight element TCAS utilizes a monopulse technique by transmitting and receiving with sum ($\sum$) and difference (Δ) beams to determine the bearing of the intruder [2]. The four element TCAS determines the direction of an intruder by transmitting a beam in one of four selectable directions [13]. In contrast to the monopulse system, this system receives the replies from the surrounding aircraft omnidirectionally. By omnidirectional, it is meant that all of the four beams are used to receive the incoming signals

where each of the four beams is connected to a different receiver. These four received signals are then processed to determine the bearing of the intruder. From here on, the eight element TCAS will be simply referred to as the 'monopulse system'; while, the four element system will be labeled as the 'amplitude system'. The study of the amplitude system is necessary because of the relatively high cost and complexity of the monopulse system.

It is shown in this paper that the simpler four element TCAS III system appears to perform fairly well when compared to the monopulse system. As expected, the simulations show that true and detected bearing of the intruder with respect to the TCAS-equipped aircraft are different due to the effects of the scatterers on the aircraft. One of the most important results of the theoretical studies are the bearing error curves. These curves are plots showing the true bearing of the intruder versus the error in detecting its bearing for various elevation angles. These error curves are used to obtain bearing rate errors, and various other parameters which are used to determine the performance of the TCAS system. In this paper, these error curves are used to compare the performance of the monopulse and amplitude systems for various locations of the antenna array along the fuselage of an aircraft. These error curves will also be used in the future as transfer functions in the simulation of encounters between a large number of aircraft where other sources of error such as noise will be taken into account.

This paper is organized as follows. In Sections 2 and 3, the simulation of the monopulse and amplitude systems will be described, respectively. In Section 4, results will be presented comparing the performance of these two system when mounted on a Boeing 737 aircraft. It is important to point out that the TCAS systems being considered by the FAA may have top as well as bottom mounted (on the fuselage) antenna arrays. In the present paper, results for only a top mounted array will be presented.

2 Eight Element Monopulse TCAS III

2.1 Principle of Operation

The TCAS III antenna for the monopulse system discussed in this paper was built by Bendix [2]. It consists of an eight element, 10.5″ diameter, electronically steered circular array with a transponder at the center. Each element is a top loaded monopole that is matched at the base by means of a microstrip network. The transponder is also top loaded and helps increase the directivity of the pattern. The TCAS system transmits interrogation signals via a sum beam and difference beams at 1030 MHz to interrogate intruders located within a 22.5° sector around boresight. By means of phase shifters, these beams can be rotated to any one of 64 equally spaced directions. An idealized example of $\sum$ and Δ beams is shown in Figure 1.

A Butler Matrix is used to create the sum and difference beams. It gives the normalized element excitations E_i of the i^{th} element for a given set of mode inputs according

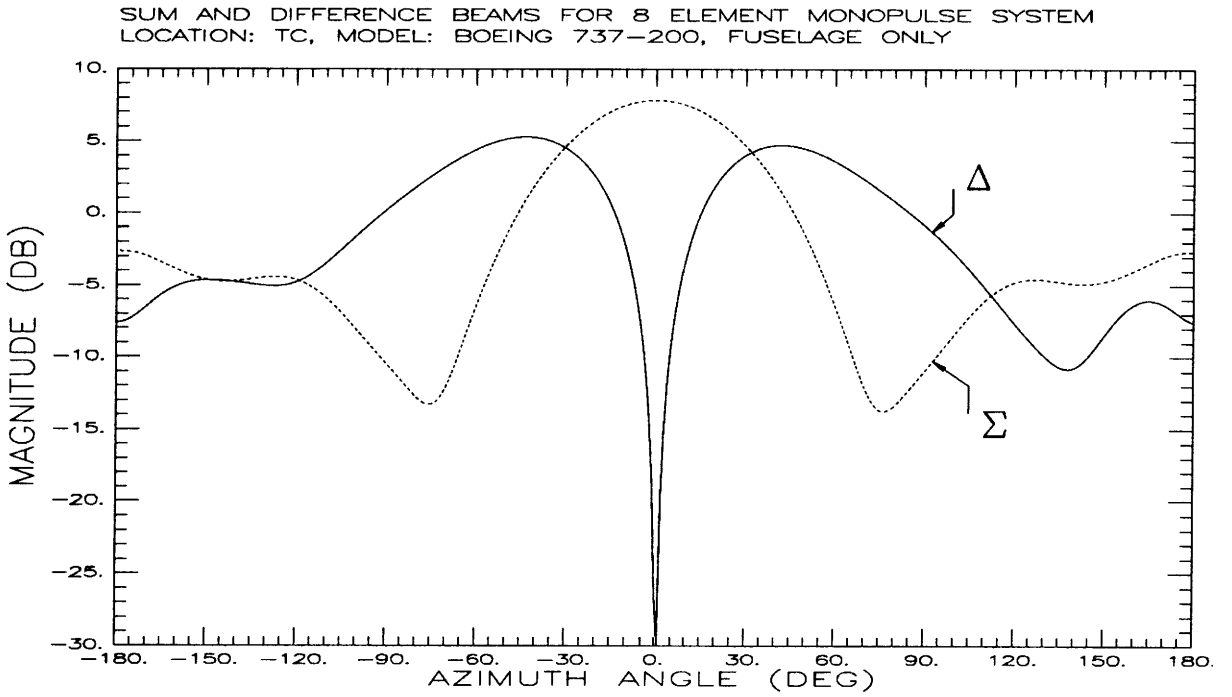

Figure 1: Sum and difference beams for TCAS mounted on the fuselage of a Boeing 737-200, 378″ from the nose.

to

$$E_i = \frac{1}{\sqrt{N}} \sum_{l=-N/2+1}^{N/2} M_l e^{j2\pi il/N} \tag{1}$$

or conversely

$$M_l = \frac{1}{\sqrt{N}} \sum_{i=1}^{N} E_i e^{-j2\pi il/N} \tag{2}$$

where E_i is the complex excitation of the i^{th} element, M_l is the complex l^{th} mode input for a given beam heading, and N is the number of elements in the array (in this case, $N = 8$).

An N element circular array of radius a is shown in Figure 2. To steer the beam α radians counterclockwise, a negative phase gradient is applied across the mode inputs such that

$$M_l = A_l e^{j(P_l - l\alpha)} \tag{3}$$

where P_l is the phase of the l^{th} mode input (radians).

The transponder on the target aircraft (intruder) replies to this query in a series of encoded pulses at 1090 MHz if the received pulse via the sum beam is stronger than

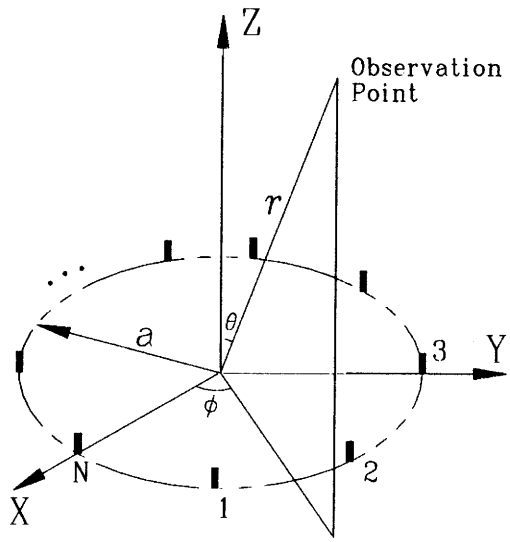

Figure 2: Geometry of an N element circular array.

that via the difference beam. This reply is fed to a Squinted Beam Monopulse Processor, which gives a monopulse curve according to

$$M = 20 \log_{10} \left| \frac{\sum + j\Delta}{\sum - j\Delta} \right| \tag{4}$$

where $\sum$ and Δ are the complex received signals via the sum and difference beams, respectively. The angle convention followed to define the elevation and azimuth angles is depicted in Figure 3. An idealized example of a monopulse curve is shown in Figure 4. To determine the actual azimuth bearing angle of a target, the processor output is compared with a lookup or calibration table. The generation of these lookup tables is discussed below.

2.2 Modeling and Simulation

When the OSU Aircraft Code [8] is used to calculate the radiation patterns of an array mounted on the fuselage of an aircraft, the antenna model should already include coupling effects (between the elements of the array) because this code does not consider this important effect. These coupling effects can be taking into account by means of a moment method analysis or by making measurements. It turns out, as shown in [5] where various models are considered for the eight monopulse TCAS array, that the pattern of a single monopole of the array radiating in the presence of the other monopoles, which are terminated in conjugate matched loads, can be simulated by a set of ideal monopoles where it is assumed that there is no mutual coupling between them. Evaluating the accuracy of various models [5], it appears that a very simple model can be used to simulate the radiation pattern of every single monopole of the monopulse circular array. This

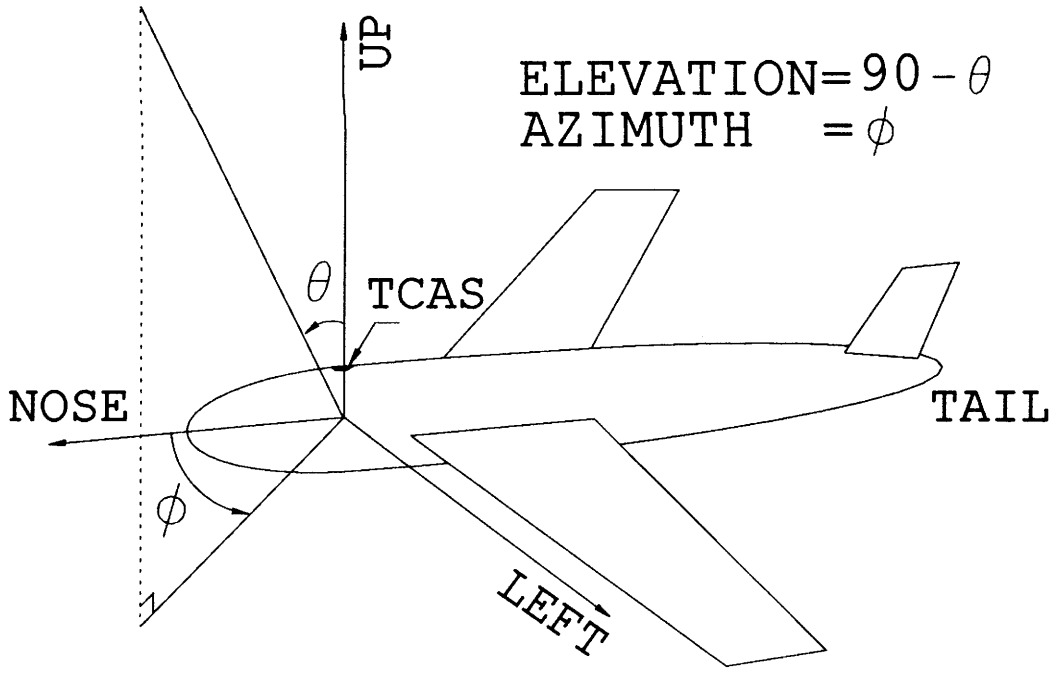

Figure 3: Definition of elevation and azimuth angles with respect to TCAS mounted aircraft.

model, depicted in Figure 5, consists of a pair of ideal monopoles separated by $\lambda/4$ and excited 90° out of phase.

The desired cardioid shape of the radiation pattern of each element of the array (this was determined by measurements conducted by Bendix) can be obtained by properly exciting the two monopoles in Figure 5. For this model, the exact phase center corresponding to radiation direction $\beta = 0$ is given by

$$x_p = \frac{1 - B/A}{1 + B/A}\lambda/8 \tag{5}$$

where A and B are the excitation weights of the outer and inner monopoles, respectively, and x_p is the phase center. The ratio A/B is adjusted to get a 16 dB front to back ratio which was also determined from measurements. The accuracy of the model described above is shown in Figure 6 where the measured patterns were obtained on a 6′ diameter curved ground plane whose curvature was same as the Boeing 727 at the antenna location [2]. The final step in the modeling of the TCAS array is to determine the phase center of each element of the circular array by means of a moment method analysis as done in [5] or by making some measurements. Once the location of these phase centers have been determined and matched with the phase center of the pair of monopoles depicted in Figure 5, the complete model of the array is obtained as shown in the same figure.

In order to estimate the bearing of an intruder, two sets of monopulse curves are created. First, the TCAS is mounted on an aircraft fuselage model without any plates. The element patterns are found from the OSU Aircraft Antenna Code from which 64

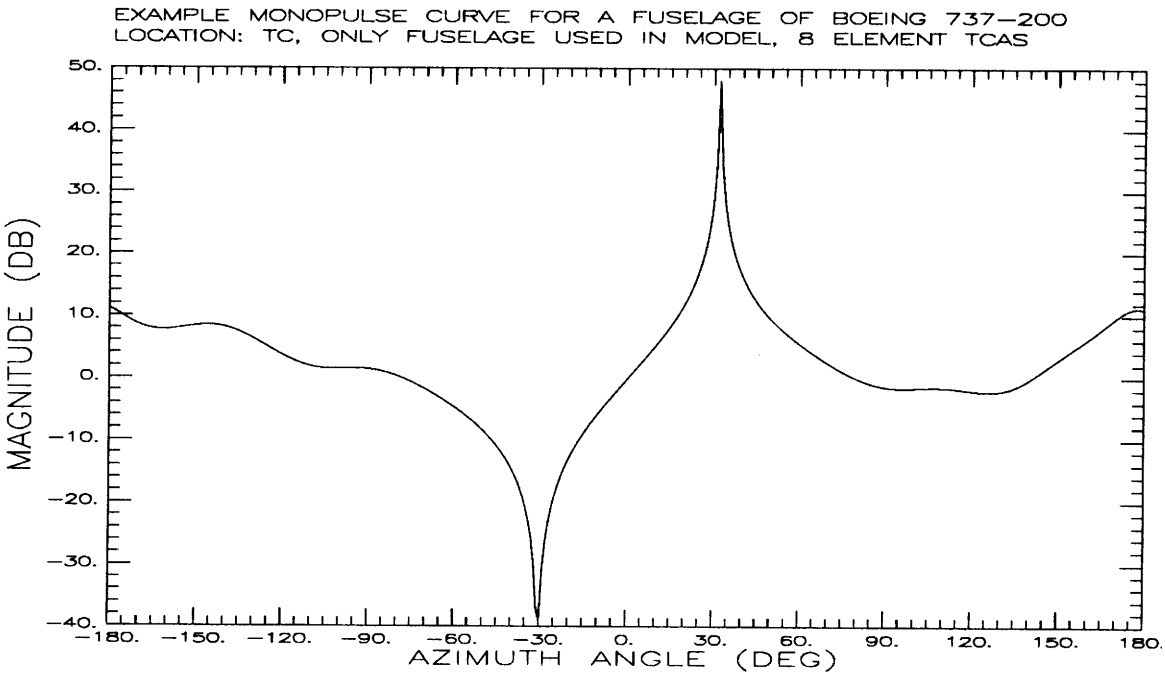

Figure 4: Idealized monopulse curve formed by the processor. The aircraft model consists only of a Boeing 737-200 fuselage.

monopulse curves are created corresponding to 64 the different bearings of the sum and difference beams. These curves are referred to as the 'lookup tables' and are used to calibrate the system. The lookup tables are created for a 10° elevation angle ($\theta = 80°$). Next, the whole aircraft is modeled including the wings, tail, engines, etc., using flat plates and the radiation patterns are obtained again, at any elevation angle of interest. Monopulse curves are created again, and these are seen to be distorted versions of lookup tables because they include the effect of scattering by the structural components. These tables are referred to as 'wing tables'.To calculate the bearing, one starts with the actual received signal using the wing table and locates this number in the lookup table. The bearing can then be determined from the lookup table. The error in estimating the bearing of the intruder is then computed as follows:

$$\epsilon = \phi_{detected} - \phi_{actual} \tag{6}$$

where ϵ is the bearing error, $\phi_{detected}$ and ϕ_{actual} are the predicted and actual bearing of the intruder, respectively. This lookup table result is illustrated in the top graph of Figure 7. By computing the error for each bearing at a specific elevation, a bearing error curve is obtained whose resolution is 1°. A typical error curve is also shown at bottom of Figure 7, which was generated for a Boeing 727 model for the 8 element TCAS array mounted 380″ from the nose. The TCAS was mounted slightly off-center, which leads to an unsymmetric error curve. As expected, the bearing error is larger in the direction of the tail (around $\pm 180°$) because of the blockage by the vertical stabilizer. The effect of

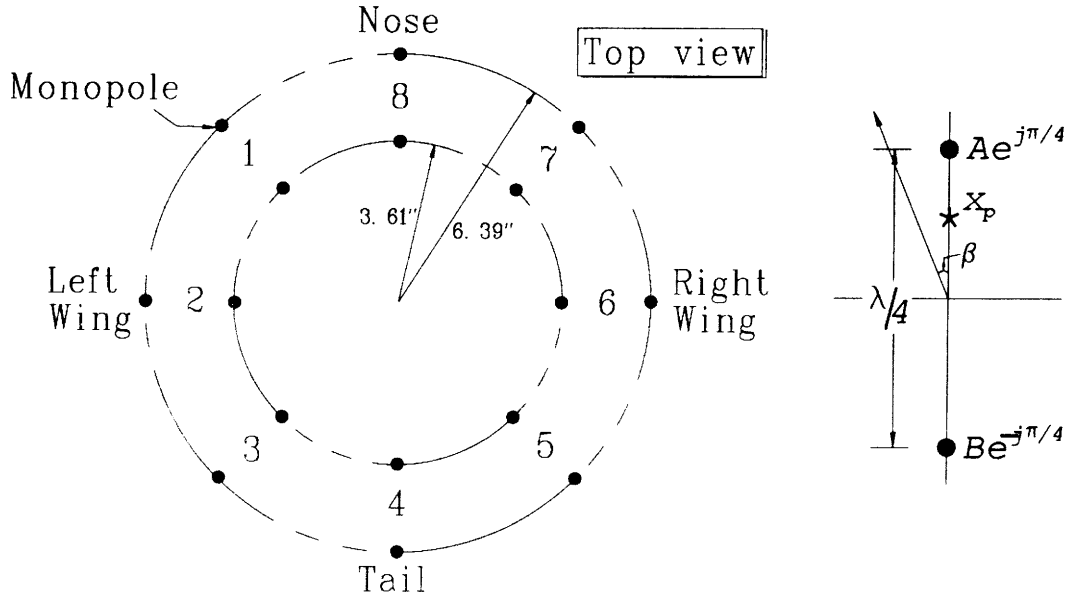

Figure 5: Two element model of TCAS III.

the wings can also be observed around $\pm 90°$; however, their effect is smaller than that due to the vertical stabilizer.

3 Four Element Amplitude TCAS System

3.1 Principle of Operation

The four element TCAS is an amplitude comparison system. In this system, the four element circular array transmits a beam in one of four selectable directions. The array is mounted on the aircraft and aligned such that the beams are directed in the directions of $0°, 90°, 180°$, and $270°$ of relative bearing, and as in the monopulse system, they are transmitted at 1030 MHz. In contrast to the monopulse system, the signal is received by all the four beams (at 1090 MHz), where each of these beams is connected to a different receiver. The magnitudes of the four received signals are then compared and the difference of the largest two is taken. This result is then compared against a calibration curve to estimate the bearing of the intruder aircraft [13].

3.2 Modeling and Simulation

The beams must have a 3-dB beamwidth of $90° \pm 10°$ and a 10-dB beamwidth of $180° \pm 10°$ for all elevation angles between $+20°$ and $-15°$ for a top mounted antenna. A sketch of the desired pattern is shown in Figure 8.

The TCAS array is modeled by four short z-directed monopoles on a ground plane with sinusoidal current distributions as shown in Figure 2, with $N = 4$ where the angular

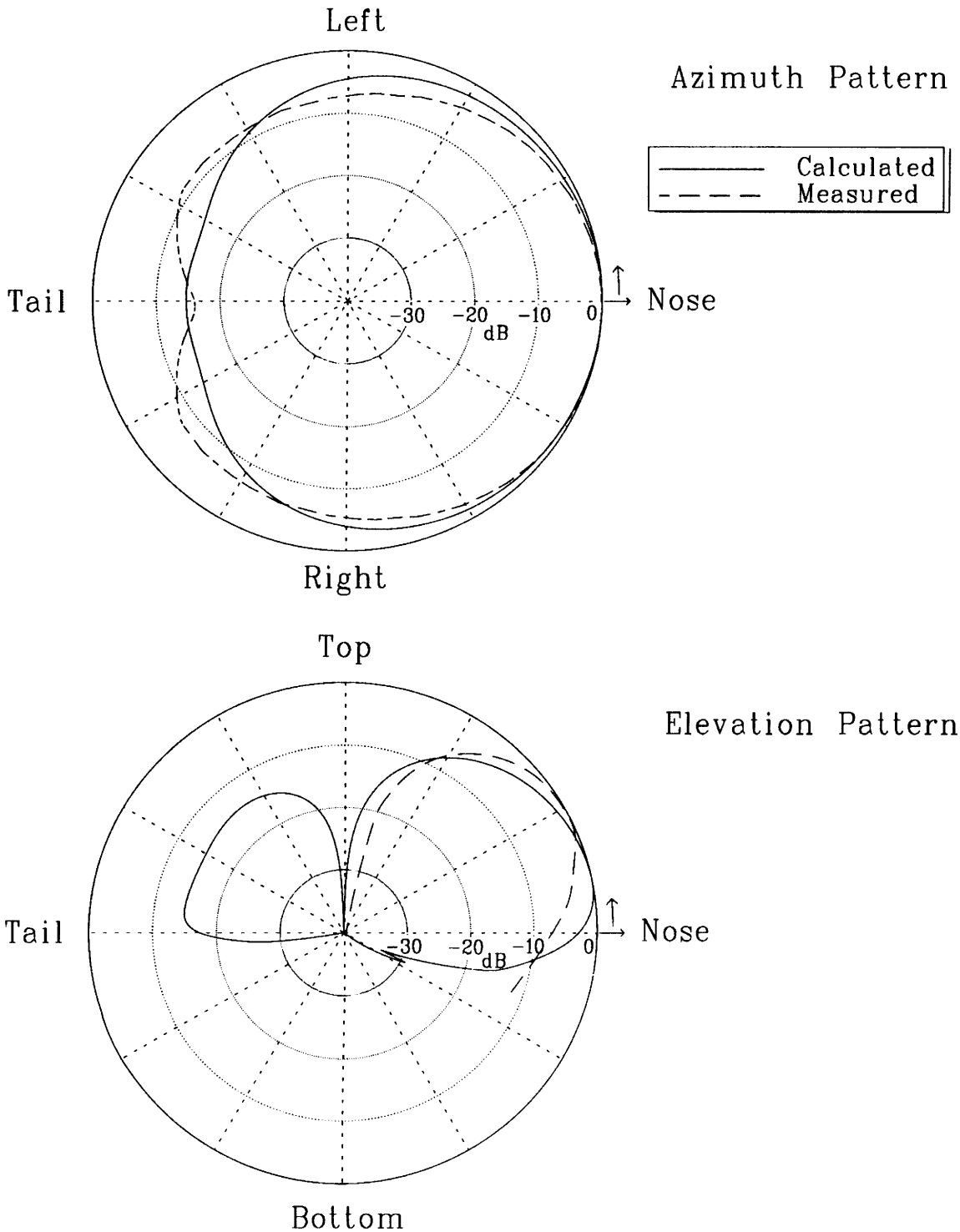

Figure 6: Calculated and measured radiation pattern of a single monopole of the TCAS array radiating in the presence of other elements of the array.

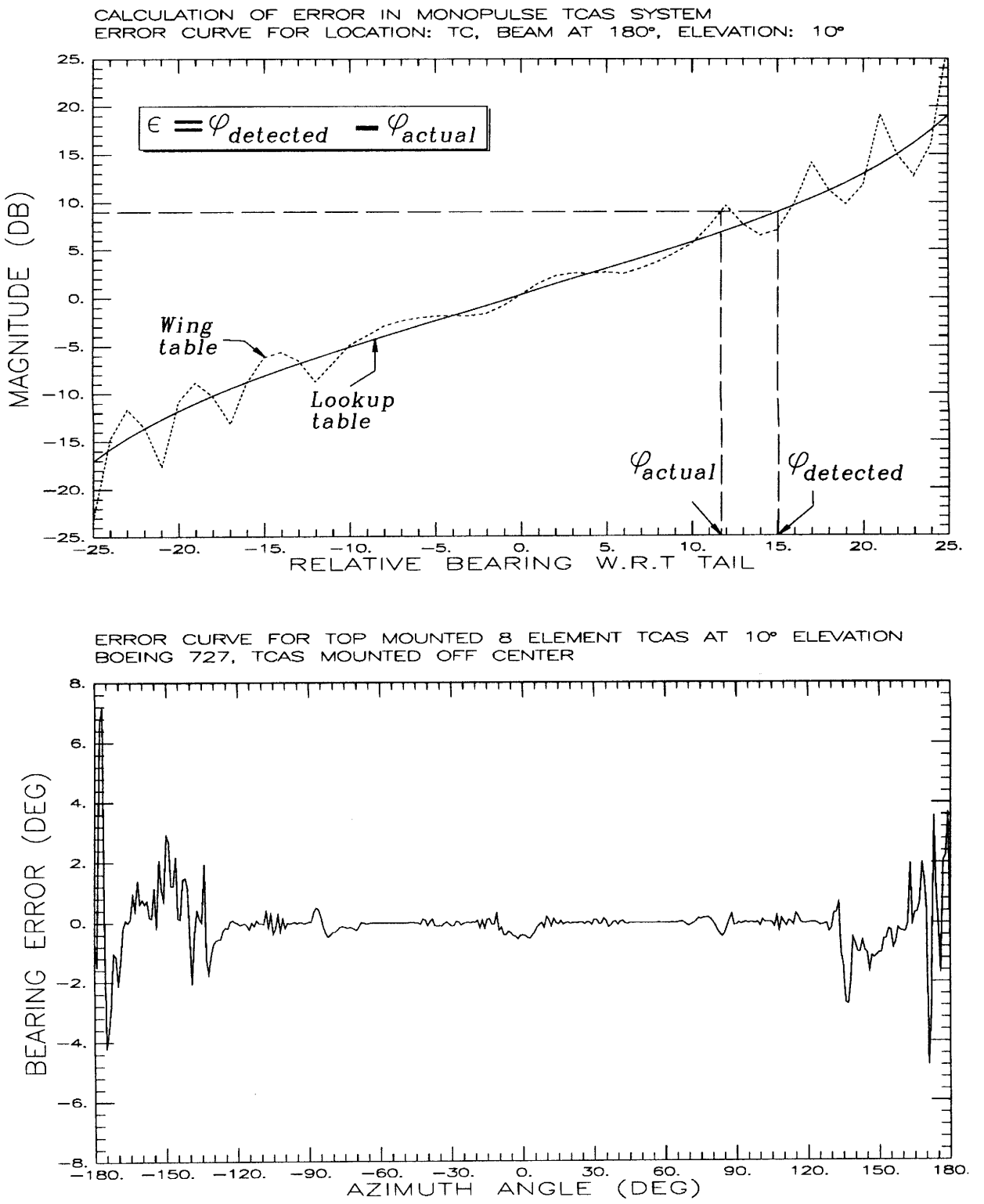

Figure 7: Procedure to calculate bearing and bearing error (top) and a typical error curve for Boeing 727 at at 10° elevation for an off-center mounted 8 element monopulse TCAS (bottom).

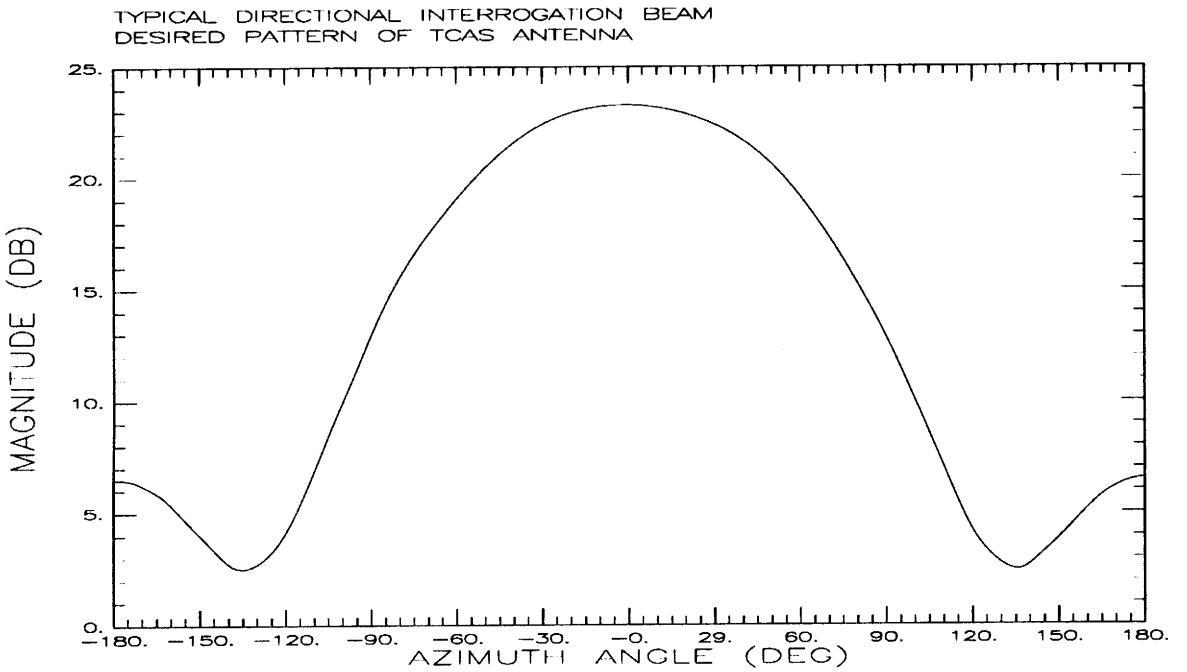

Figure 8: Desired antenna pattern for four element TCAS.

location of the i^{th} element is $\phi_i = i90°$ $(i = 1, 2, 3, 4)$. Let the excitation of the individual elements be given by

$$I_i = A_i e^{j\alpha_i} \tag{7}$$

where I_i is the complex excitation, A_i is the amplitude and α_i is the phase of the i^{th} element, respectively. The elements are counted counterclockwise from the X-axis (nose direction) as shown in Figure 2.

The far field antenna pattern $E_\theta(\theta, \phi)$ is the product of the element pattern $\mathrm{F}(r, \theta, \phi)$ and the array factor $\mathrm{AF}(\theta, \phi)$ such that

$$E_\theta(\theta, \phi) = \mathrm{F}(r, \theta, \phi)\mathrm{AF}(\theta, \phi). \tag{8}$$

Note that the element pattern $\mathrm{F}(r, \theta, \phi)$ will be calculated by the OSU Aircraft Antenna Code [8, 9], whereas the array factor is given by

$$\mathrm{AF}(\theta, \phi) = \sum_{i=1}^{4} A_i e^{j(\alpha_i + ka\sin\theta\cos(\phi - \phi_i))} \tag{9}$$

where k is the free space wavenumber, and all other symbols have been defined earlier.

Since the number of elements is small $(N = 4)$, the amplitudes are set to a constant value $A_i = A$, and only the phase of the excitation is modified so as to get a maximum in any one of the four given directions given by $\phi_j = j90°$ $(j = 1, 2, 3, 4)$, corresponding to left, tail, right and nose directions, respectively. Also, to have a symmetrical pattern, the two elements perpendicular to the axis of the beam heading must have the same phase.

From these requirements, for example, for a beam maximum in the direction of the nose ($\theta = \theta_0, \phi_j = 360°$), one must have

$$\begin{aligned} \alpha_4 &= \text{arbitrary} \\ \alpha_1 &= \alpha_4 + ka \sin\theta_0 \\ \alpha_2 &= \alpha_4 + 2\,ka \sin\theta_0, \text{ and} \\ \alpha_3 &= \alpha_1. \end{aligned} \tag{10}$$

The weights were calculated for each beam heading $\phi_j = j90°$ and for $\theta_0 = 80°$, because $\theta_0 = 80°$ corresponds to the elevation angle of most interest, namely 10°. These weights are then kept fixed in all further calculations.

As expected, when the antenna was mounted on the fuselage of an aircraft and studied, it was found that the beam maxima are no longer identical to each other. Furthermore, the radius of the array was varied slightly to obtain the best agreement between the ideal and calculated patterns. For this study, $a = 2.31''$ and $l = 2.78''$ were used, where l is the length of the monopole.

In the simulation, the TCAS antenna is mounted on the fuselage without any structural components and the received signals are calculated at various bearings. The azimuthal space is divided into four quadrants; namely, 0°–89°, 90°–179°, 180°–269°, and 270°–359°. Under ideal circumstances, the two channel numbers of the highest beams in each quadrant are known and one of these is selected as the reference signal. The other signal is subtracted from this reference signal to obtain a 'lookup table'. Since there are four beam directions, there are four monotonically increasing sections of the lookup table as shown in Figure 9. This table also stores the channel numbers of the two beams that generated any particular value of the lookup table. The table that lists the channel numbers and the reference signal for all possible ϕ is given in Table 1.

ϕ (degrees)	Highest Channel	Next Channel	Reference Beam
0–44	1	2	
45–89	2	1	2
90–134	2	3	
135–179	3	2	3
180–224	3	4	
225–269	4	3	4
270–314	4	1	
315–359	1	4	1

Table 1: Reference beams for the TCAS under ideal conditions.

Next, the various scatterers like wings, stabilizers etc., are added to the fuselage which leads to variations in the amplitude of the signals being received. Again, the difference signal is computed and stored along with the channel numbers in the 'wing table'. To

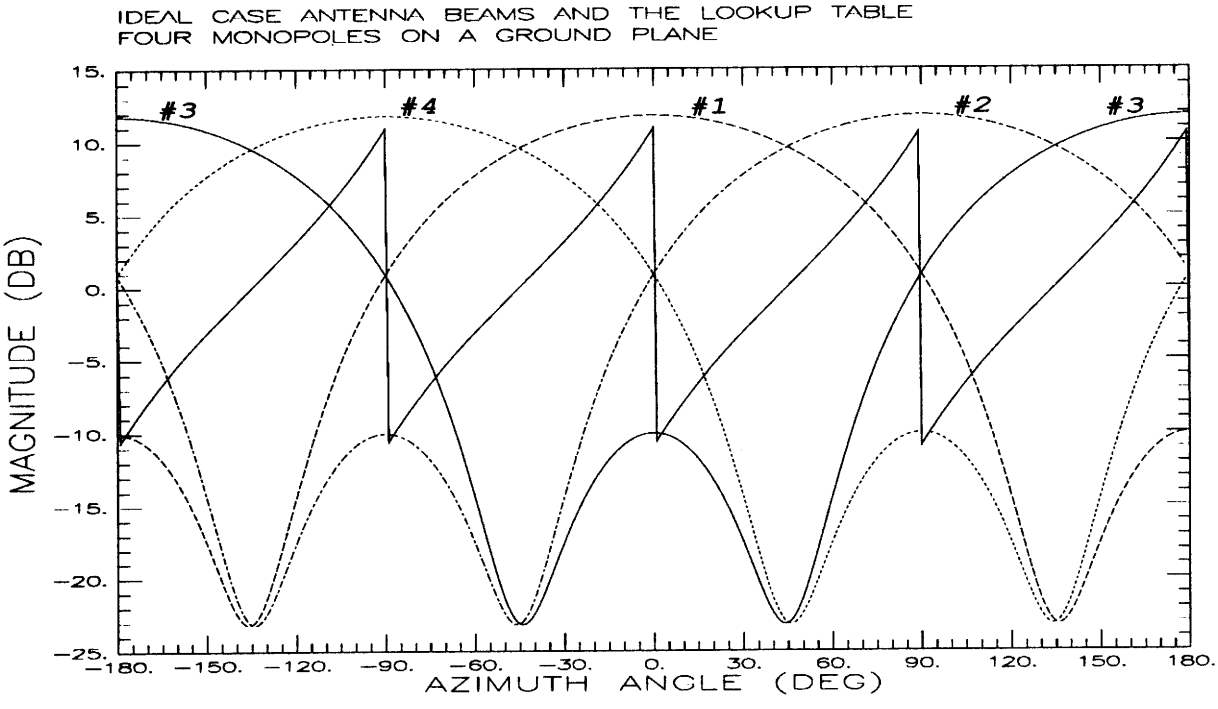

Figure 9: Creation of receiver beams and the lookup curve.

calculate the bearing, one starts with a given difference signal, the corresponding set of two highest received signals and their respective channel numbers for the case when the aircraft is simulated with wings, etc. From the channel number of the reference beam, one can place the intruder in one of the four quadrants. That section of the lookup table is then searched for the same value of difference signal as illustrated in Figure 10. A linear interpolation scheme is used to find the predicted bearing when the difference signal lies between two points in the lookup table. The bearing error ϵ is then calculated as before, i.e., $\epsilon = \phi_{detected} - \phi_{actual}$.

There are two sources of error that arise here. If the difference signal lies outside the range of the lookup table; i.e., the two highest received signals are a valid combination of beams but the value of the difference signal is not within the boundaries of the corresponding section of the lookup table. Then, an 'out of range' warning is generated as shown in Figure 10 and the bearing is set to the extreme value of the lookup curve. Another type of error occurs when two beams that have opposite bearings are received as the highest signals because of the scattering by the various structures of the aircraft. This leads to an illegal combination of channels and one cannot calculate a table entry for this ϕ. This leaves the processor with no lookup table to search and the bearing of the intruder cannot be estimated. The error is then set equal to the previous value of error and a 'no lookup table' warning is given and the plot is marked accordingly [13].

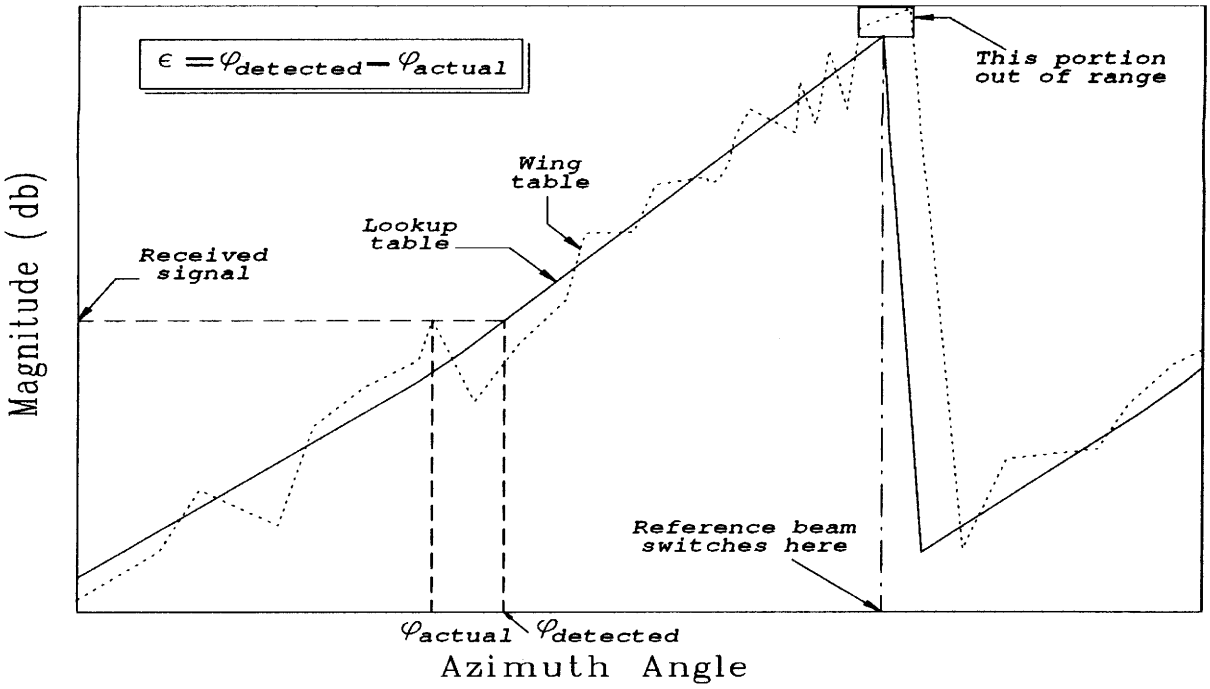

Figure 10: Calculation of bearing and bearing error.

4 Results and Discussion

Results are provided for the case of a top mounted TCAS (on a Boeing 737-200) antenna based on the algorithms described above. The engines were not included in the model because they are far from the antenna and are shadowed by the fuselage (see Figure 11). The horizontal stabilizer was also not included in the model because it does not affect the radiation patterns for the locations and elevation angles considered here. Although the engines are not included in the present analysis, they cannot be ignored for a bottom mounted TCAS as reported in [13].

The total field $\bar{E}^t$ radiated by each element of the two TCAS arrays considered here is calculated by adding the fist order Uniform Theory of Diffraction (UTD) field components depicted in Figure 12, namely

$$\bar{E}^t = \bar{E}^s + \bar{E}^r + \bar{E}^d + \bar{E}^c \tag{11}$$

where $\bar{E}^s$ is the source field (Figures 12a, b), $\bar{E}^r$ is the reflected field (Figure 12c), $\bar{E}^d$ is the edge diffracted field (Figure 12d, e) and $\bar{E}^c$ is the corner diffracted field (Figure 12f). For the kind of geometry and antenna locations considered in this paper, (11) is sufficient to accurately calculate the radiated field. However, if necessary, higher order UTD field components such as reflected-reflected fields, reflected-diffracted fields etc., can be added to the total field in (11) [9]. Note that the OSU Aircraft code [8] has also the capability to calculate these higher order terms.

The results in this section show the error in estimating the bearing of the intruder

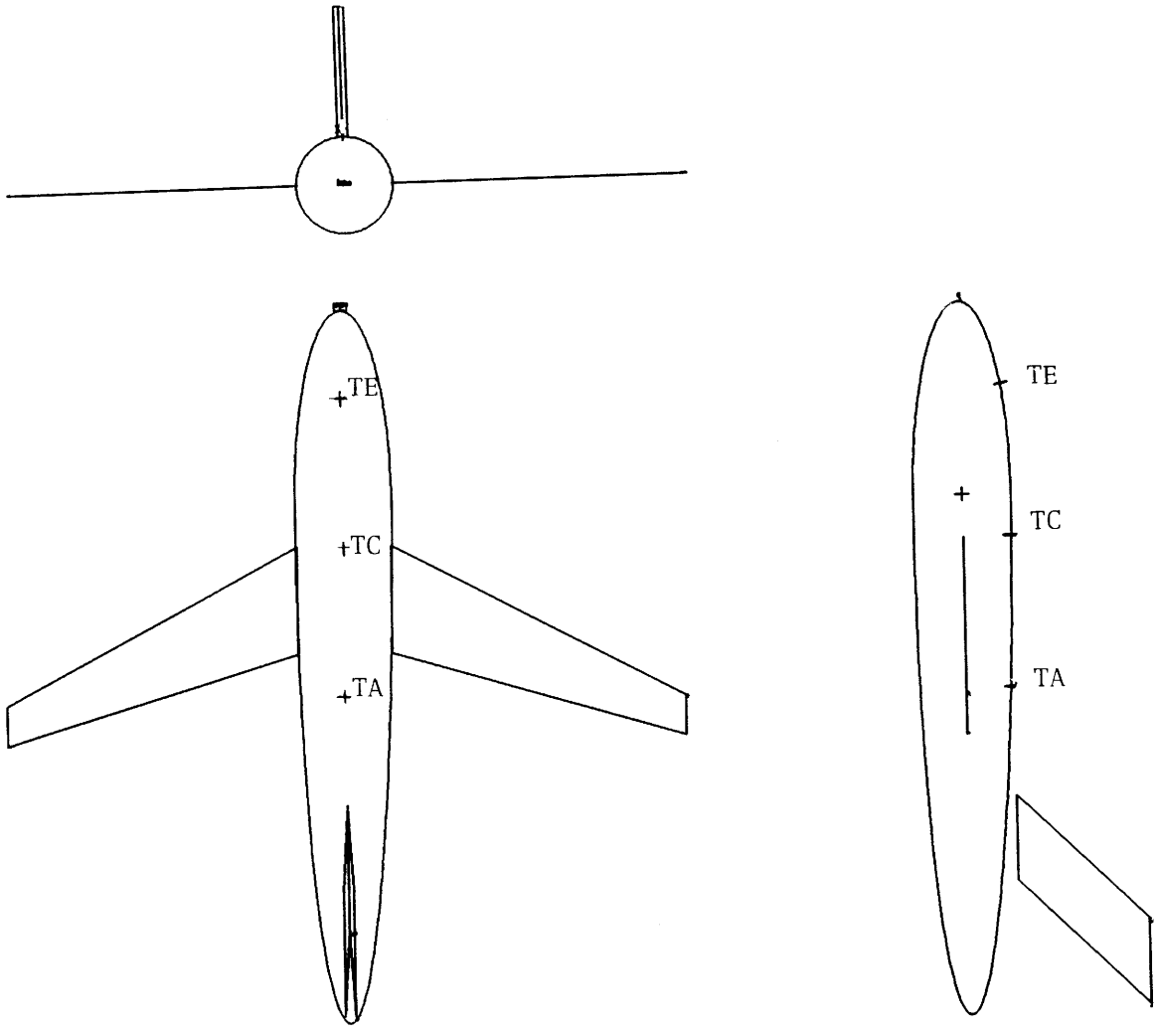

Figure 11: Model of Boeing 737-200 for a top mounted TCAS antenna.

when the TCAS is mounted on top of a Boeing 737-200 at three locations. The headers in these plots also contain some useful information for quick reference. The first line of the header gives the number of elements in the antenna system (eight or four), the location of TCAS (i.e., top or bottom mounted), and the name of the airplane modeled, respectively. The second line gives the location of antenna and the elevation angle. Third line gives information about the distance of antenna from the nose any other relevant information about the model. Notice that the plots are all antisymmetric about 0°.

The error curves for four element TCAS are also marked where the previously discussed error conditions occur. The locations of TCAS used here are labeled TA, TC, and TE (where 'T' denotes a top mounted antenna). The details about these locations are tabulated in Table 2 and views of the model are given in Figure 11. Error curves are provided for three elevations: +20°, +10°, and 0° for the monopulse as well as amplitude system. The main reason for doing this is to compare the performance of both systems. Obviously, the computer model of the aircraft and the antenna location is the same for both systems.

One feature that is observed in some of the error curves for the four element amplitude

Antenna Location	Distance from nose (inches)
TA	618.6
TC	378.6
TE	138.6

Table 2: Locations of TCAS on top of Boeing 737-200.

system are the jumps which are absent from the eight element monopulse system error curves. This seems to be an inherent problem in the operation of the amplitude system. It can be shown that the jump in the error curves occurs because of the slight change of the beams as a function of elevation and also because of the beam switching technique used to calculate the bearing. This can be seen more clearly in the top graph of Figure 13 where two calibration or lookup curves calculated at 10° and 20° are shown. If one calculates an error curve where the calibration curve at 10° is used as a reference and the calibration curve at 20° as the received signal, the result is an error curve which is discontinuous at $-90°$, 0°, 90°, and 180° as illustrated in bottom picture of Figure 13. A similar calculation also shows that there is no discontinuity in some of the error curves, especially those close to the elevation for which the lookup table was created. This is probably the most serious drawback of the four element system. One possible solution is to generate lookup tables for various elevation angles instead of just one elevation angle which is done in the monopulse system. Note that, in all the results shown here, the lookup tables were generated for only a 10° elevation angle.

At location TA, which is 618.6″ from the nose, for an elevation of 20° the error curve for the four element TCAS shown in Figure 14 meets the specifications ($|\epsilon| < 2°$) only in the nose quadrant; however, except for the jump at 0°, its performance in this quadrant is slightly better than the eight element TCAS mounted at the same location. The performance of the amplitude comparison system is not as good as the monopulse system in the left and right quadrants. This is because, the four element TCAS antenna transmits beams in the directions 90° and 270° where they are distorted by the wings. The eight element monopulse system also transmits a sum beam in these directions, however, unlike the four element TCAS it also transmits a difference beam. Note that both systems perform poorly in the tail quadrant due to the presence of the vertical stabilizer. At an elevation of +10° (see Figure 15) the statistics show that the TCAS III performs much better in the left and right quadrants (collectively called the 'side' quadrants from here on), in addition to the nose quadrant. The maximum error of the monopulse and amplitude systems is well within the 2° limit in the nose quadrant. In the tail region, both systems fail due to the scattering by the vertical stabilizer.

At 0° elevation (Figure 14), the 4 element amplitude system is slightly better than the 8 element monopulse system in the nose quadrant. However, the 8 element monopulse system still performs better in the side quadrants. The statistics of error for the tail region are similar. There is some similarity in the shape of the two error curves; however,

the ripples in the error curve are usually more pronounced for the amplitude system.

Next, at location TC, which is 378.6″ from the nose the monopulse system is better than the amplitude system in all quadrants at 20° of elevation as depicted in Figure 16. Again, one notices the jumps in the error curve (for the 4 element array) for an elevation of 20°, which is not present in the 8 element system. It is also found that the maximum error is much higher for the four element TCAS in the nose quadrant. For an elevation of 10°, the performance of the amplitude system is very similar to that of the monopulse system as shown in Figure 17. In the nose quadrant, both systems meet the specifications very well. These observations also hold for a 0° elevation angle for both antennas as seen in Figure 16; however, the amplitude system is somewhat better than monopulse system in the nose quadrant. The errors in the tail quadrant are too great for either system to be of much use. The 4 element TCAS also exhibits higher error in the side quadrants.

Finally, at TE, which is closest to the nose at 138.6 inches, the 4 element TCAS does not meet the requirements at 20° elevation as depicted in Figure 18. The error curve is also discontinuous at all beam switching angles. The error curve for the 8 element monopulse system is smooth and the performance of the system is more acceptable. At 10°, however, both antennas perform well in the nose quadrant. Further, the monopulse system meets the specifications in the side quadrants also as opposed to the 4 element TCAS (see Figure 19). At 0° elevation, the monopulse system is still better than the amplitude version in the nose quadrant where its performance is acceptable. This is not the case for 4 element TCAS whose performance at this location is not very good. The error parameters of both antennas in other quadrants also indicate that the monopulse system performs better at this location for 0° elevation as shown in Figure 18.

The performance of the four element TCAS is generally not as good as the eight element TCAS III, except in the nose quadrant. This is mainly due to the method used for direction finding. The four element TCAS is more sensitive to the various structural scatterers of an airplane. The beam switching technique and the slight variation of the four query beams as a function of elevation also gives rise to the jumps referred to above. In order to minimize these jumps, it is necessary to choose an optimum length of the monopulse radiator such that the radiation pattern does not change much as a function of elevation. Furthermore, it may be necessary to generate lookup tables for various elevation angles. On the other hand, the eight element system operates on a monopulse principle which utilizes both a maximum and a null in the approximate direction of the intruder to locate it more accurately. The discontinuities seen in the four element system error curve are also absent. It seems that in directions where there are no scatterers, both systems perform well; however, in directions where there are scatterers; i.e., right, left and tail quadrants, the monopulse system performs better.

The performance of the 4 element TCAS is acceptable ($|\epsilon| \leq 2°$) in the forward direction for the locations TA and TC within the elevation range 0°–10°. It is found that in case of location TE, the location closest to the nose, the error in the amplitude system is too great for 0° elevation. The error is minimum for elevation of 10° because that is the angle at which the lookup table was created and, as the elevation gets higher or lower, the errors increase. Another observation is that the tables for the 4 element amplitude

system tend to get 'out of range' more often when the elevation angle is small. The 'no lookup table' error is more serious. This usually occurs for low elevation intruders mostly in the tail region. At these low elevations, the scattering by the various structures of the aircraft become more significant.

In summary, it is evident that both antennas are similar in performance in the nose quadrant and usually meet the specifications in the vicinity of 10° elevation. Note that the nose quadrant is the region of most interest because the collision avoidance system is primarily supposed to prevent head-on collisions. In all cases considered, the 8 element TCAS III is better than the 4 element TCAS in the side quadrants; however, both antennas are comparable in the tail region. An advantage of the 4 element amplitude system is that it is simpler than the monopulse system and therefore less expensive to build.

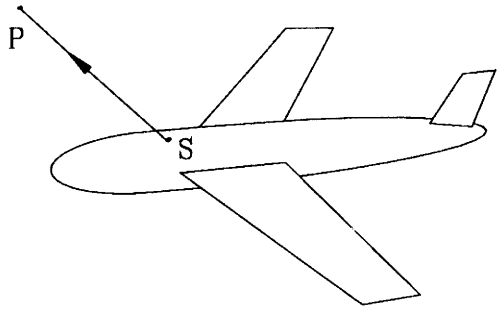

(a) DIRECT SOURCE FIELD

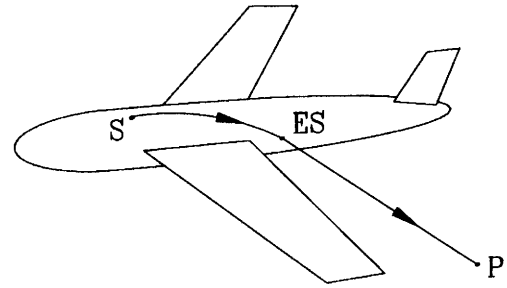

(b) EFFECTIVE SOURCE FIELD

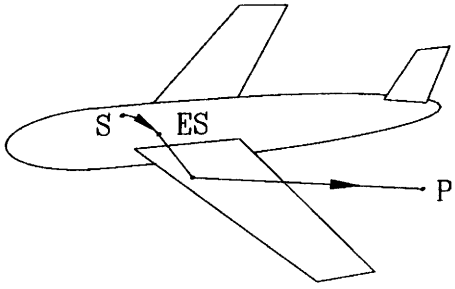

(c) REFLECTED FIELD

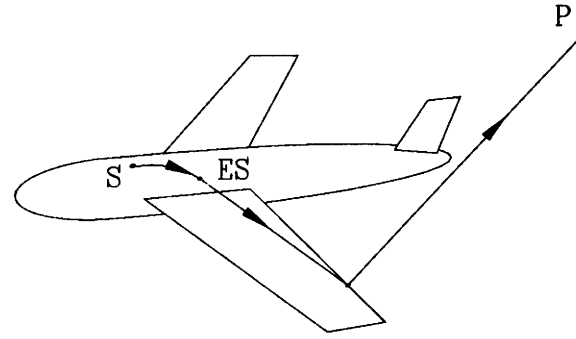

(d) EDGE DIFFRACTED FIELD

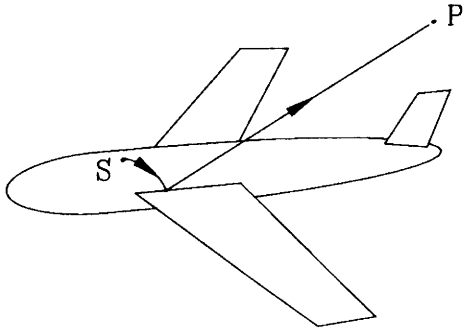

(e) CURVED JUNCTION EDGE DIFFRACTED FIELD

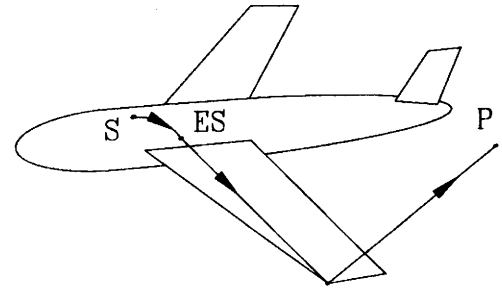

(f) CORNER DIFFRACTED FIELD

Figure 12: First order UTD field components.

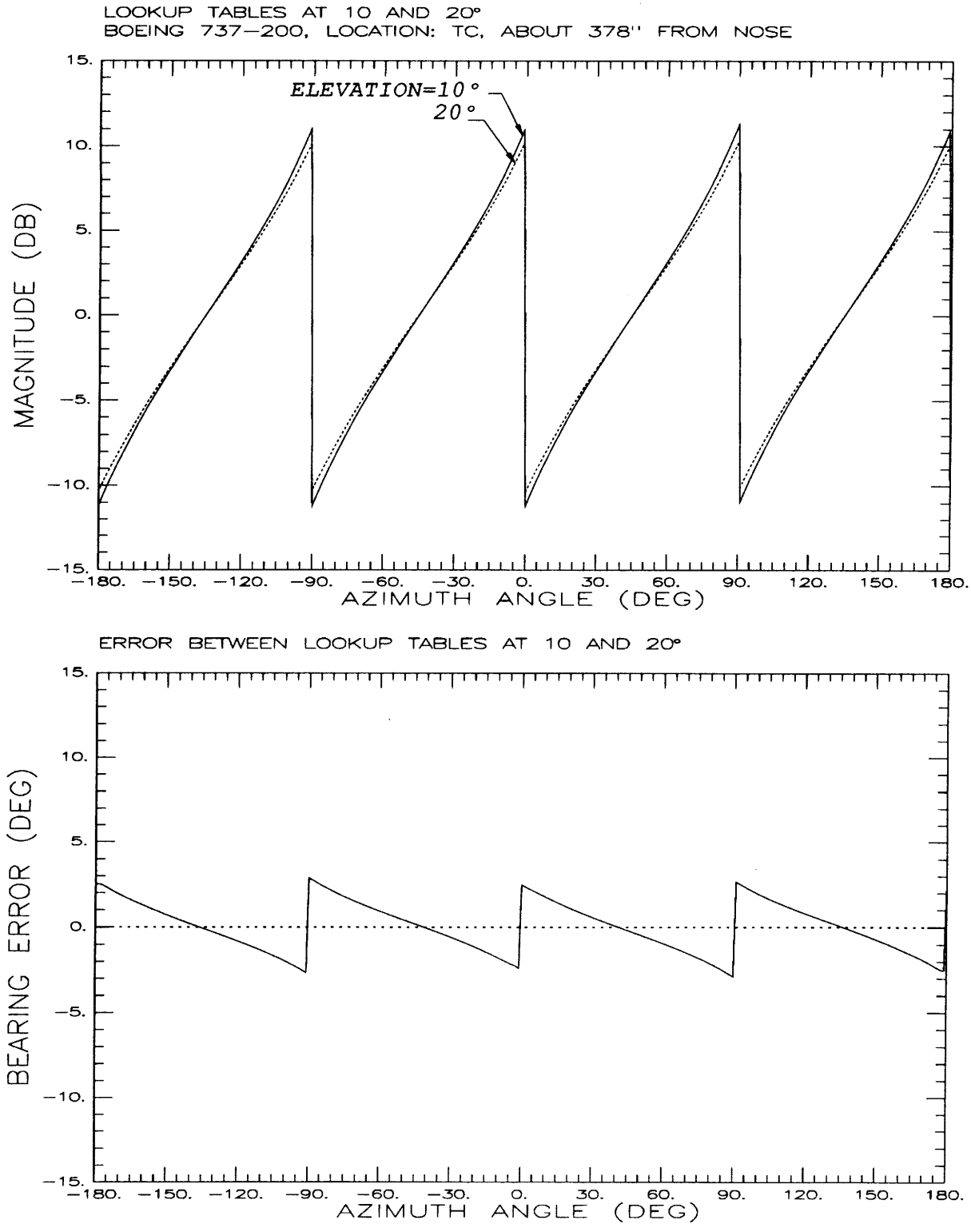

Figure 13: Explanation for jumps in the error curve for 4 element TCAS. Data corresponds to location TC.

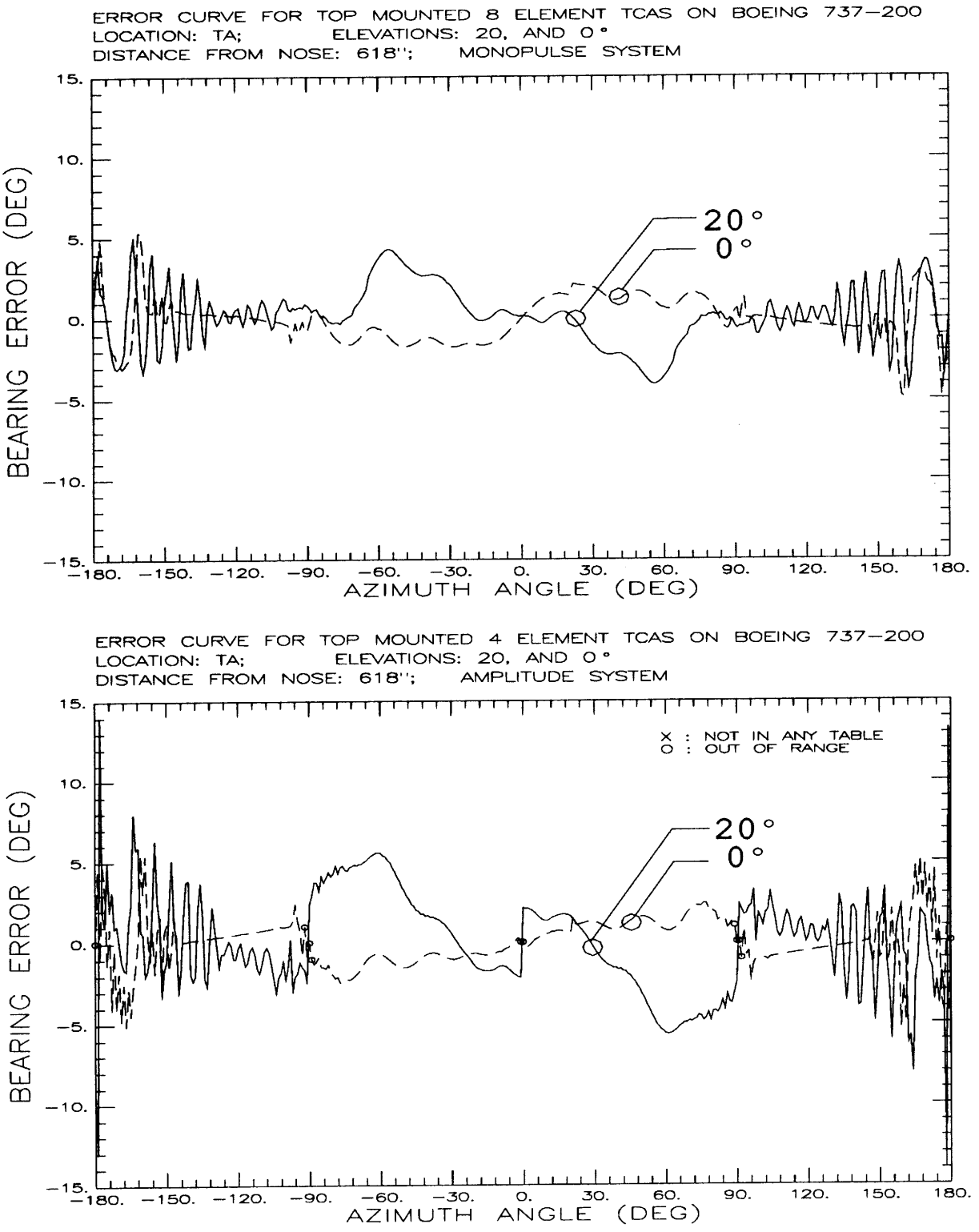

Figure 14: Error curves for 8 (top) and 4 (bottom) element TCAS at TA about 618.6″ from nose at +20° and 0°.

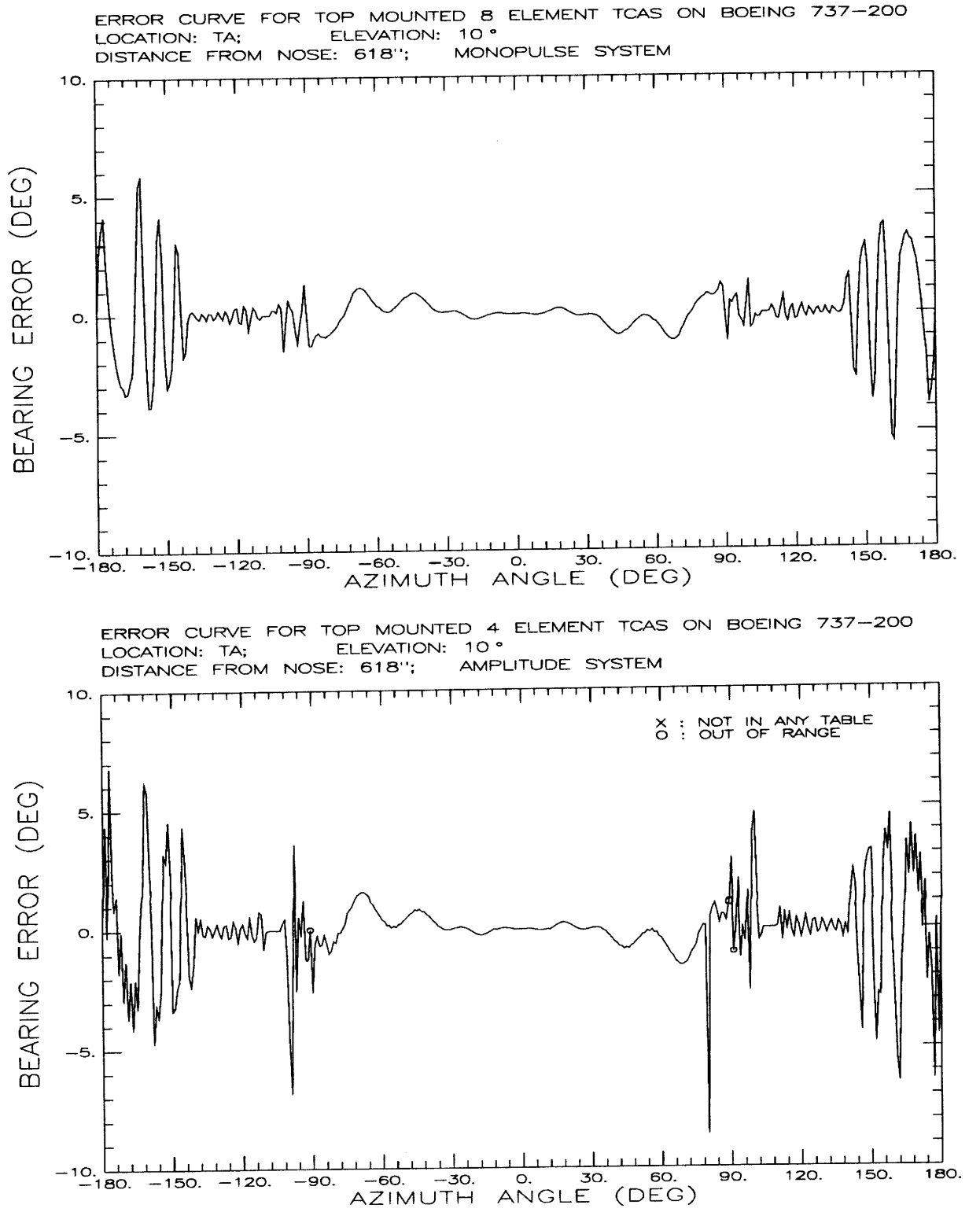

Figure 15: Error curve for 8 (top) and 4 (bottom) element TCAS at TA about 618.6″ from nose at +10°.

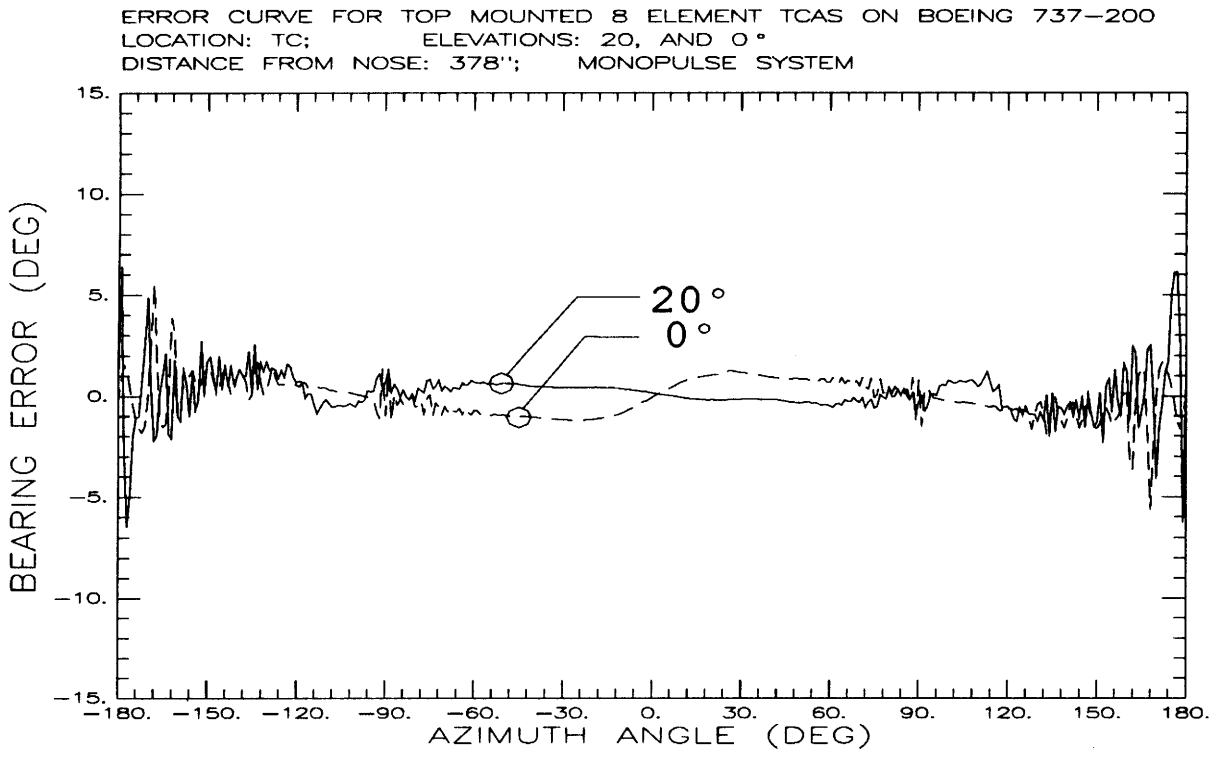

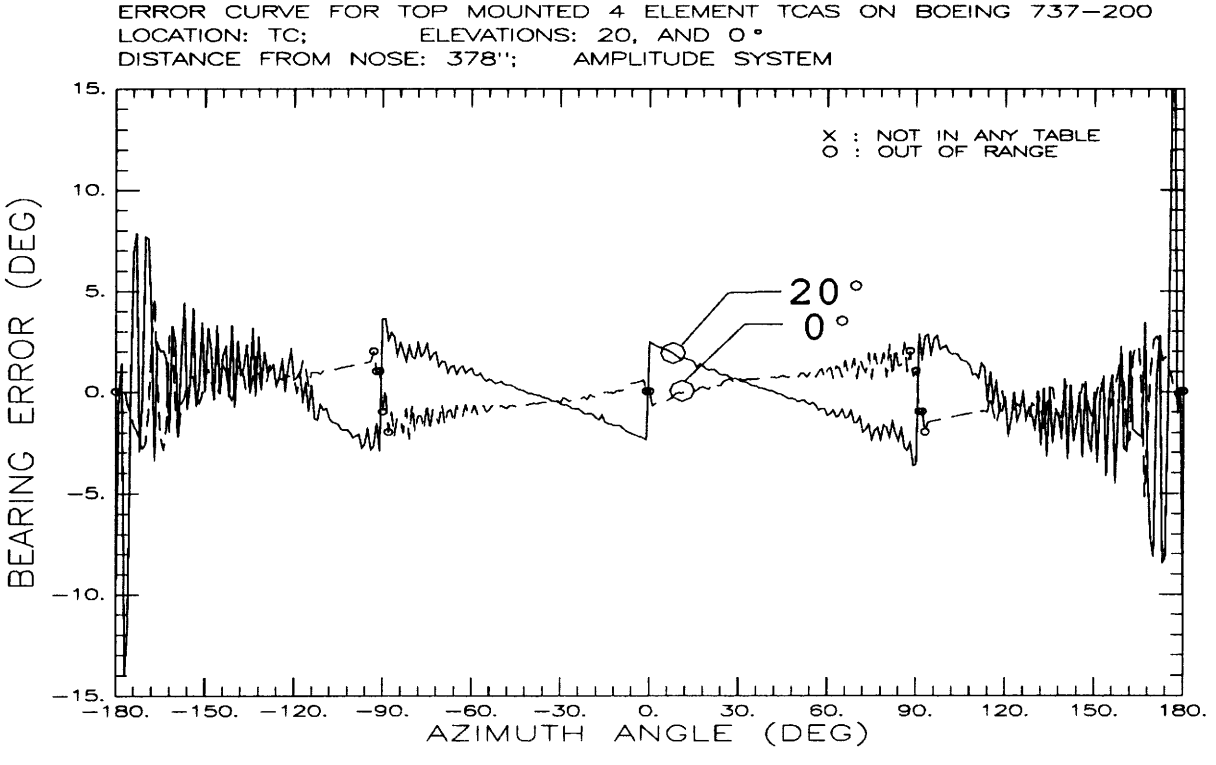

Figure 16: Error curve for 8 (top) and 4 (bottom) element TCAS at TC about 378.6″ from nose at +20° and 0°.

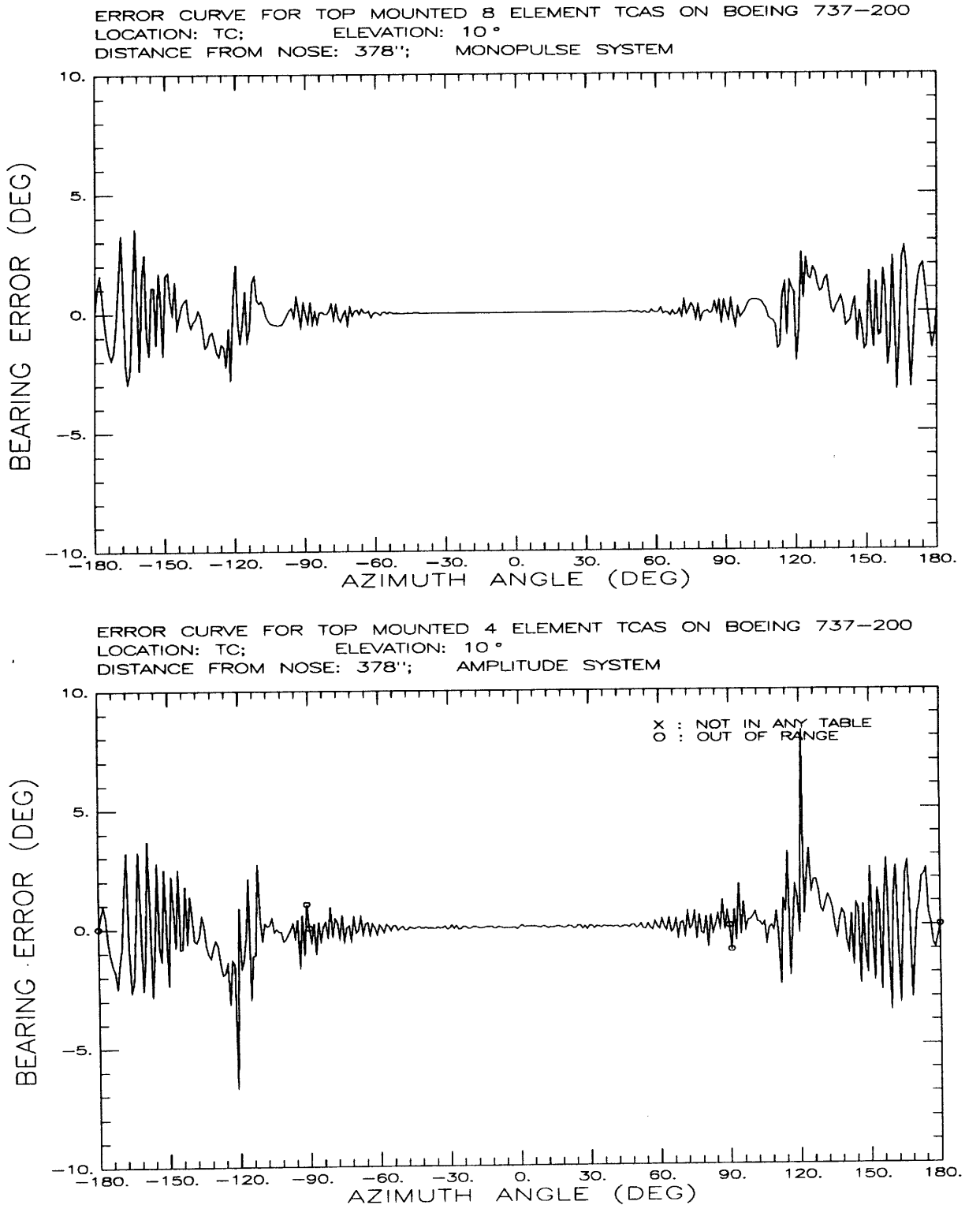

Figure 17: Error curve for 8 (top) and 4 (bottom) element TCAS at TC about 378.6″ from nose at +10°.

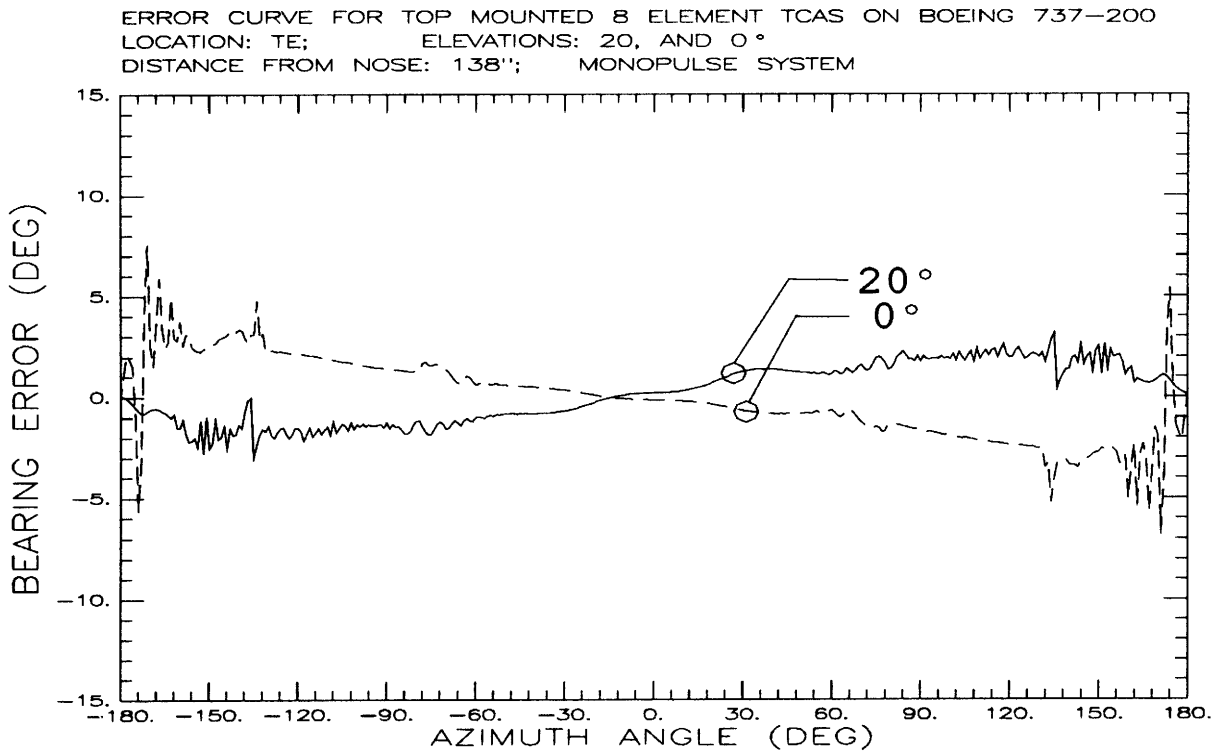

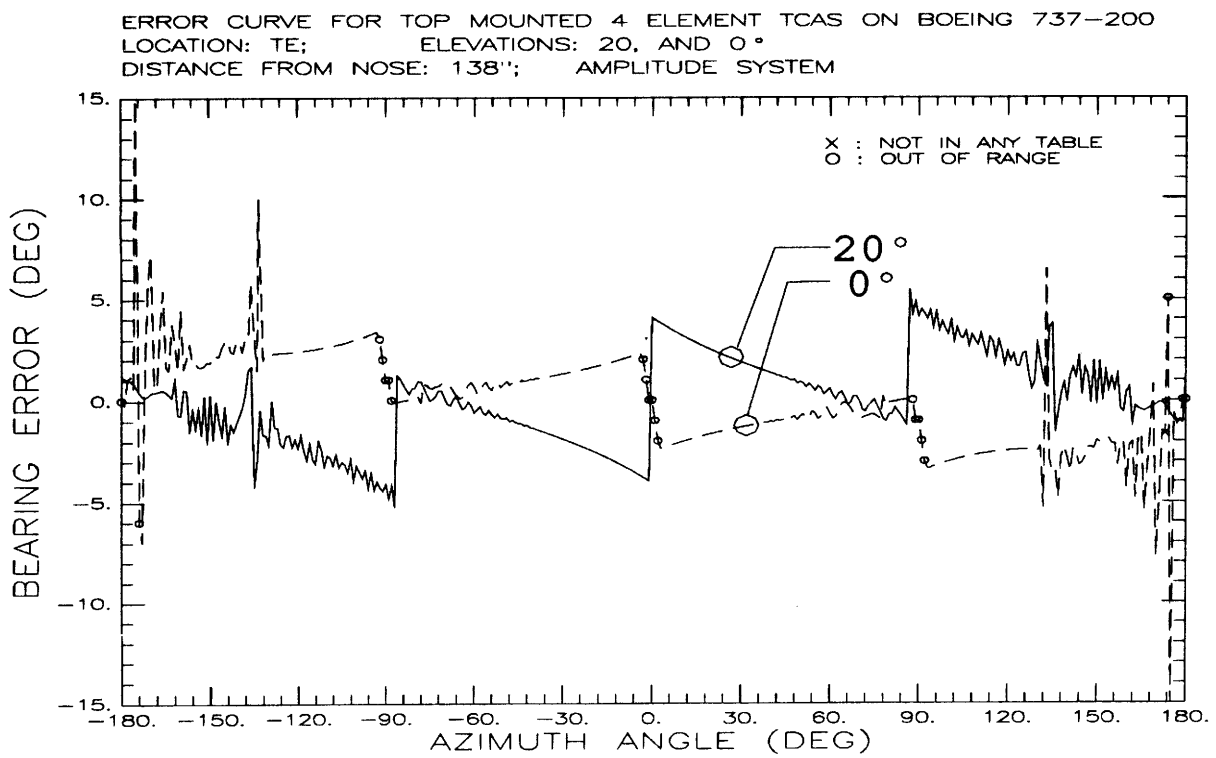

Figure 18: Error curve for 8 (top) and 4 (bottom) element TCAS at TE about 138.6″ from nose at +20° and 0°.

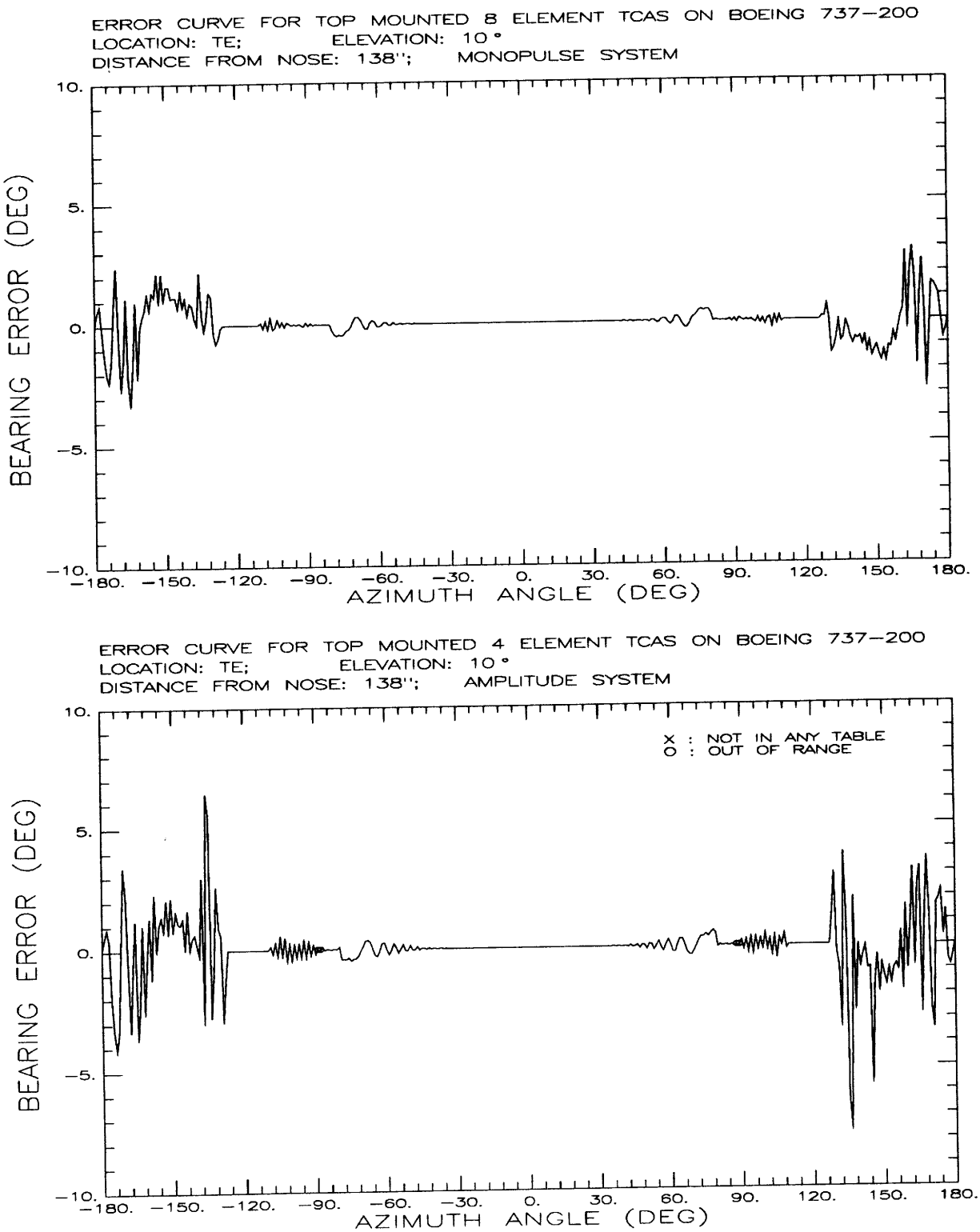

Figure 19: Error curve for 8 (top) and 4 (bottom) element TCAS at TE about 138.6″ from nose at +10°.

References

[1] E. E. Murphy, "FAA Requires U.S. Airlines to Install TCAS II by 1992." News item in The Institute, Mar. 1989.

[2] A. I. Sinsky, J. E. Reed, and J. Fee, "Enhanced TCAS II Tracking Accuracy," in *Proc. AIAA/IEEE Digital Avionics Systems Conference*, pp. 577–585, Dec. 1984. Paper 84-2738-cp.

[3] R. G. Rojas, P. H. Law, and W. D. Burnside, "Simulation of the Enhanced TCAS II System in Operation," Report 716199-9, The Ohio State University ElectroScience Laboratory, Oct. 1987.

[4] P. H. Law, W. D. Burnside, and R. G. Rojas, "A Study of a Collision Avoidance System Mounted on a Curved Ground Plane," Report 716199-8, The Ohio State University ElectroScience Laboratory, Mar. 1986.

[5] R. G. Rojas, Y. C. Chen, and W. D. Burnside, "Improved Computer Simulation of TCAS III Circular Array Mounted on an Aircraft," Report 716199-12, The Ohio State University ElectroScience Laboratory, Apr. 1989.

[6] A. I. Sinsky and R. J. Tier, "System Angle Accuracy Prediction," Tech. Rep. BCD-TN-82-035, Bendix Communicatin Division, July 1982.

[7] K. J. Kunachowicz, "Model Testing of Airborne VHF Direction Finding Antenna System," in *Antennas for Aircraft and Spacecraft*, IEE Conf. Pub. No 128, pp. 223–227, 1975.

[8] W. D. Burnside, J. J. Kim, B. Grandchamp, R. G. Rojas, and P. H. Law, "Airborne Antenna Radiation Pattern Code User's Manual," Report 716199-4, The Ohio State University ElectroScience Laboratory, Sept. 1985.

[9] J. J. Kim and W. D. Burnside, "Simulation and Analysis of Airborne Antenna Radiation Patterns," Report 716199-1, The Ohio State University ElectroScience Laboratory, Dec. 1984.

[10] W. D. Burnside, M. C. Gilreath, R. J. Marhefka, and Y. C. Yu, "A Study of KC-135 Aircraft Antenna Patterns," *IEEE Trans. Antennas Propagat.*, vol. AP-23, pp. 319–316, May 1975.

[11] C. L. Yu, W. D. Burnside, and M. C. Gilreath, "Volumetric Pattern Analysis of Airborne Antennas," *IEEE Trans. Antennas Propagat.*, vol. AP-26, pp. 636–641, Sept. 1978.

[12] W. D. Burnside, N. Wang, and E. L. Pelton, "Near Field Pattern Analysis of Airborne Antennas," *IEEE Trans. Antennas Propagat.*, vol. AP-28, pp. 318–327, May 1980.

[13] K. S. Sampath, R. G. Rojas, and W. D. Burnside, "Modelling and Performance Analysis of Four and Eight Element TCAS," Report 716199-15, The Ohio State University ElectroScience Laboratory, Apr. 1990.